

# Cascade amplifying synergistic effects of chemo-photodynamic therapy using ROS-responsive polymeric nanocarriers

Chun-Yang Sun<sup>1,1</sup>, Ziyang Cao<sup>2,1</sup>, Xue-Jun Zhang<sup>3</sup>, Rong Sun<sup>4</sup>, Chun-Shui Yu<sup>1,\*</sup>, and Xianzhu Yang<sup>2,\*</sup>

<sup>1</sup> Department of Radiology and Tianjin Key Laboratory of Functional Imaging, Tianjin Medical University General Hospital, Tianjin 300052, P.R. China

<sup>2</sup> Institutes for Life Sciences, School of Medicine and National Engineering Research Center for Tissue Restoration and Reconstruction, South China University of Technology, Guangzhou, Guandong 510006, P. R. China

<sup>3</sup> School of Medical Imaging, Tianjin Medical University, Tianjin 300203, P.R. China

<sup>4</sup> School of Biological and Chemical Engineering, Zhejiang University of Science & Technology, Hangzhou, Zhejiang 310023, P. R. China

<sup>1</sup> These authors contributed equally.

E-mail: [chunshuiyu@tjmu.edu.cn](mailto:chunshuiyu@tjmu.edu.cn) (C. S. Yu), [yangxz@scut.edu.cn](mailto:yangxz@scut.edu.cn) (X. Z. Yang)

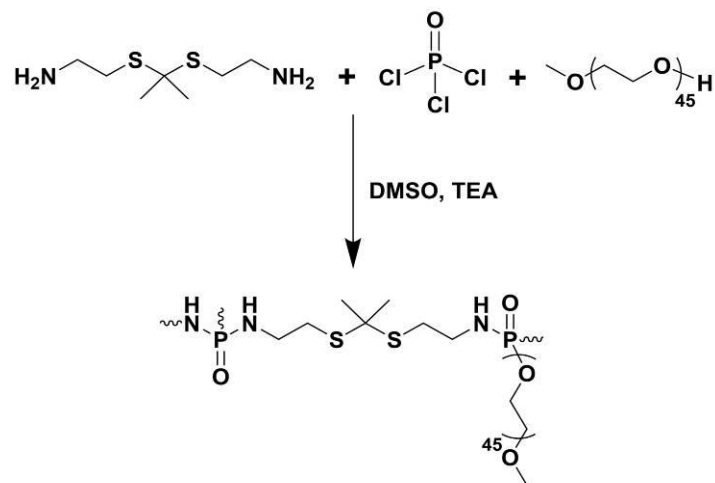


**Figure S1.** Synthetic route of hyperbranched polyphosphate (RHPPE).

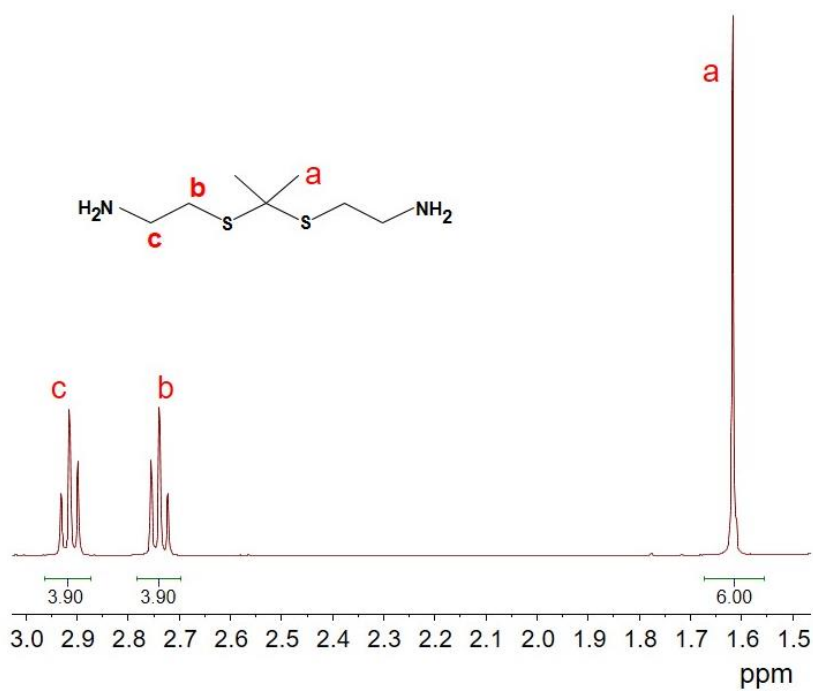


**Figure S2.**  $^1\text{H}$  NMR spectrum of RHPPE in  $\text{CDCl}_3$  recorded on an AVANCE III 400 MHz spectrometer at 25  $^\circ\text{C}$  (ppm).

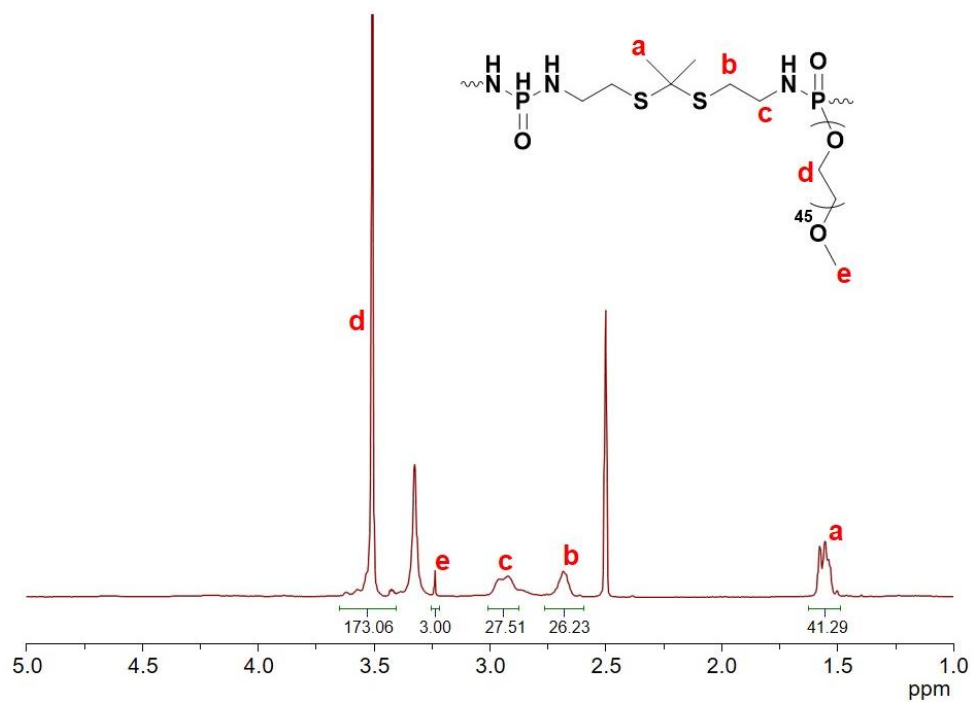


**Figure S3.**  $^1\text{H}$  NMR spectrum of RHPPE in  $d_6$ -DMSO recorded on an AVANCE III 400 MHz spectrometer at 25  $^\circ\text{C}$ .

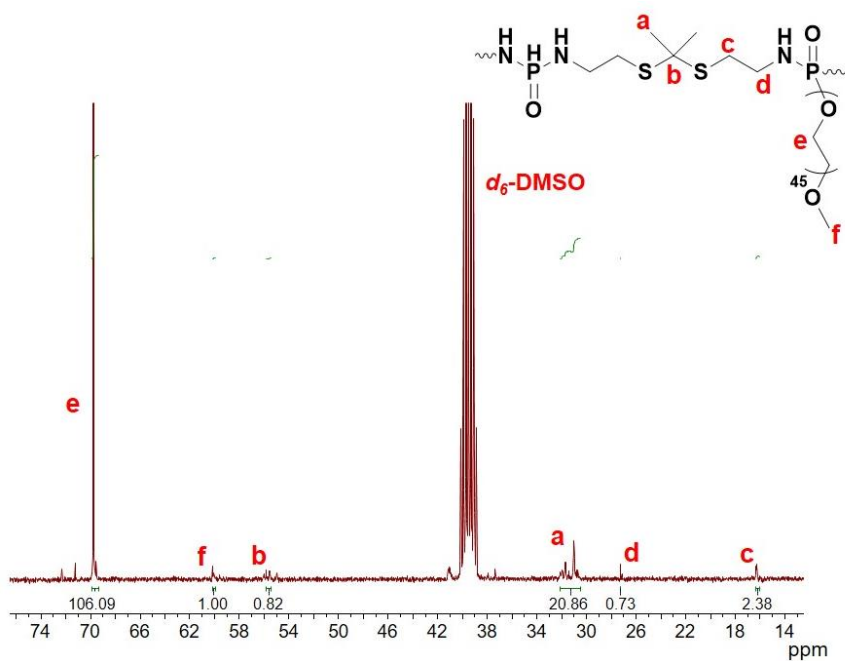


**Figure S4.**  $^{13}\text{C}$  NMR spectrum of RHPPE in  $d_6$ -DMSO recorded on an AVANCE III 400 MHz spectrometer at 25  $^\circ\text{C}$ .

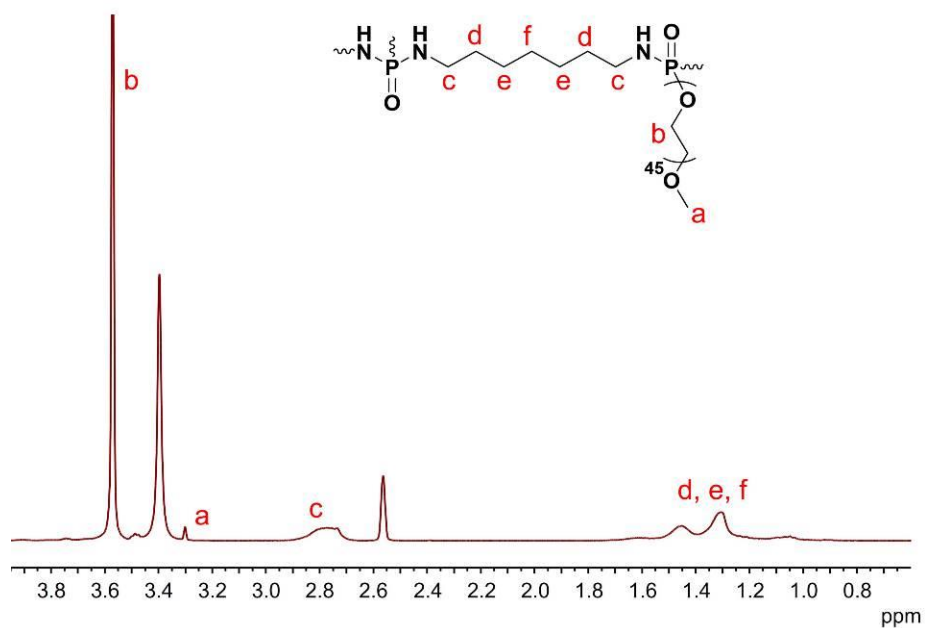


**Figure S5.**  $^1\text{H}$  NMR spectrum of non-responsive hyperbranched polyphosphate (HPPE) in  $d_6$ -DMSO recorded on an AVANCE III 400 MHz spectrometer at 25  $^\circ\text{C}$ .

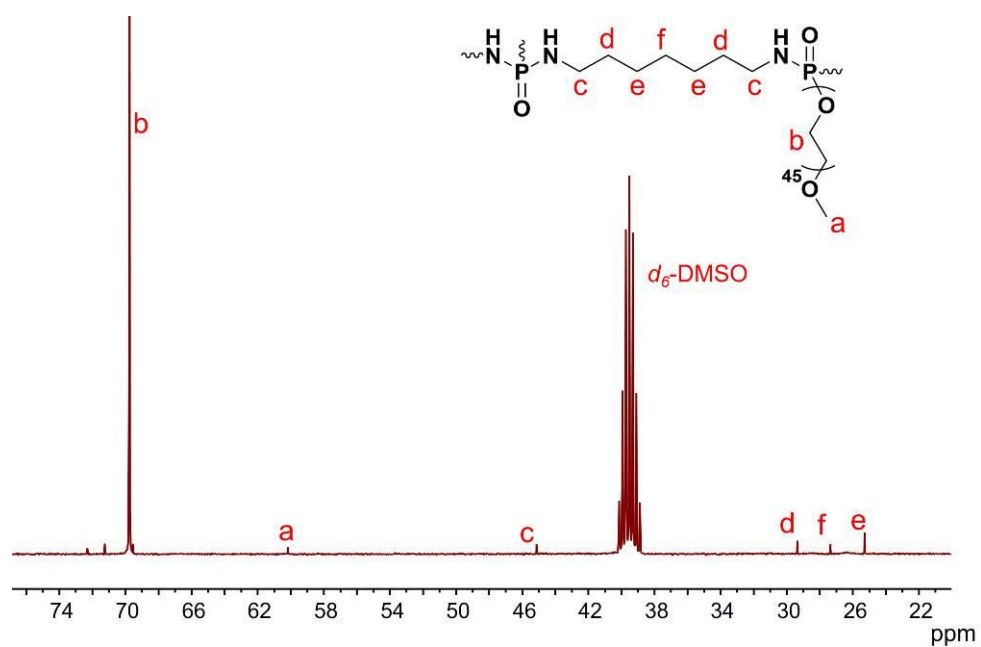


**Figure S6.**  $^{13}\text{C}$  NMR spectrum of HPPE in  $\text{CDCl}_3$  recorded on an AVANCE III 400 MHz spectrometer at 25  $^\circ\text{C}$ .

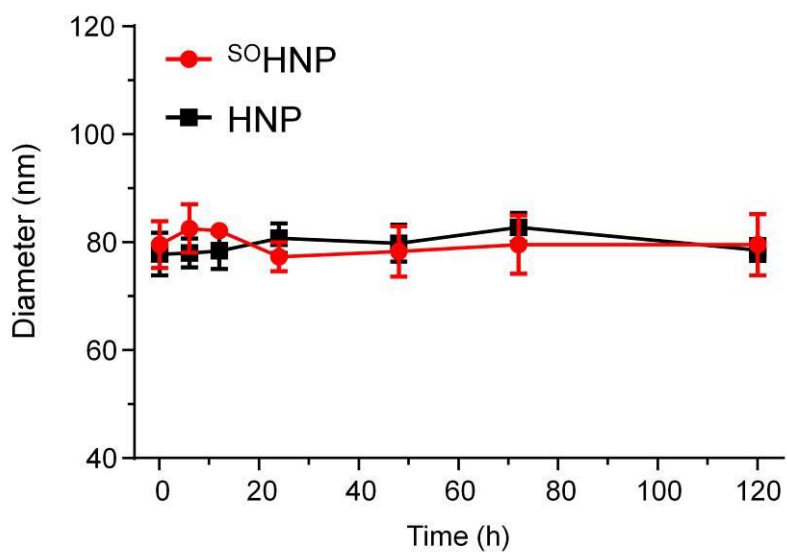


**Figure S7.** Diameter changes of  $^{SO}HNP$  or HNP as a function of incubation time in PB buffer (pH 7.4).

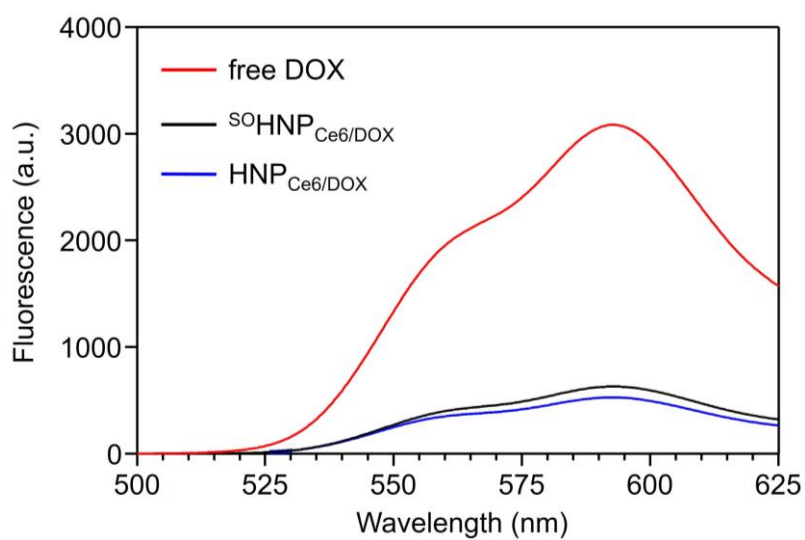


**Figure S8.** Emission spectra of free DOX,  $^{SO}HNP_{Ce6/DOX}$  or  $HNP_{Ce6/DOX}$  in aqueous solution ( $E_x=460$  nm).

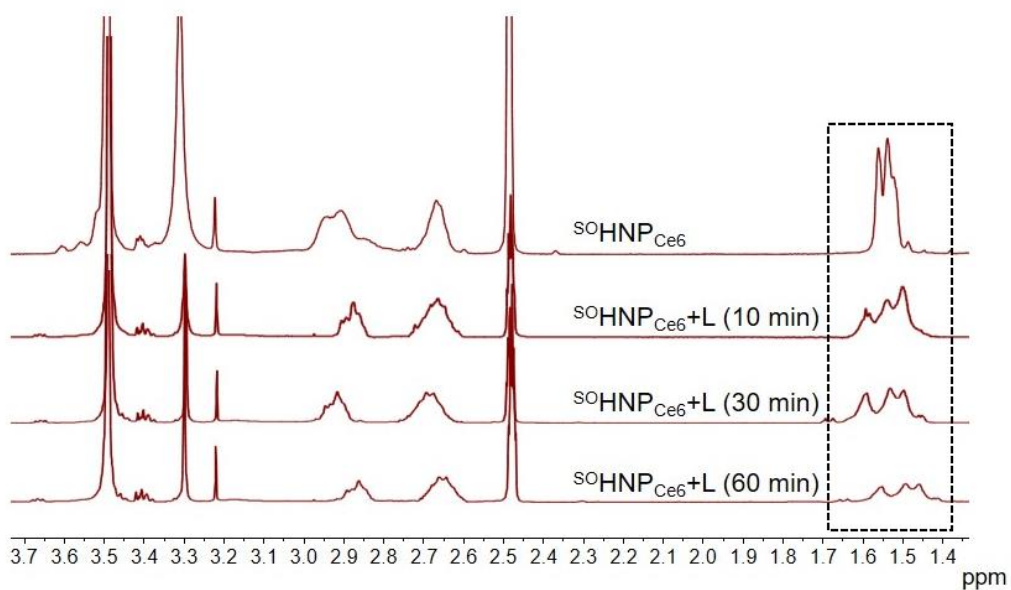


**Figure S9.** <sup>1</sup>H NMR spectra of <sup>SO</sup>HNP<sub>Ce6</sub> after 660 nm laser irradiation for different times (10, 30, and 60 min) at power intensity of 0.2 W/cm<sup>2</sup>.

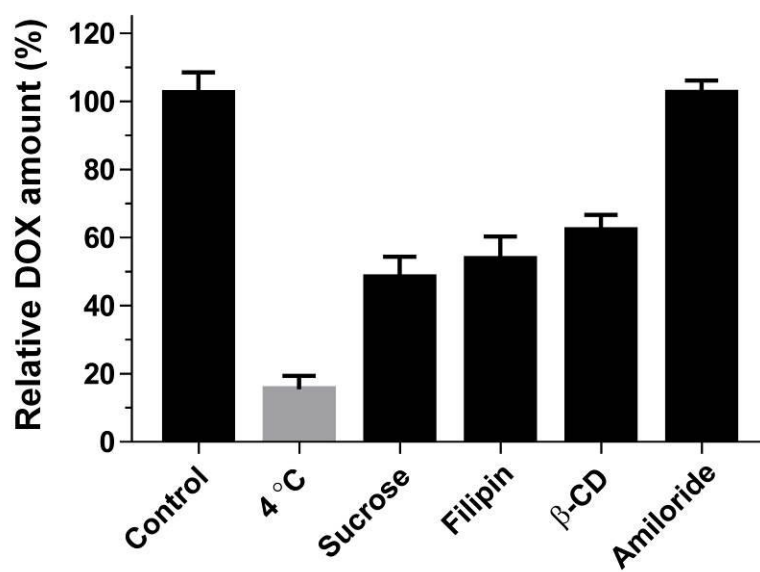


**Figure S10.** Cellular amount of DOX in MCF-7/ADR cells after 6 h of incubation with <sup>SO</sup>HNP<sub>Ce6</sub>/DOX.

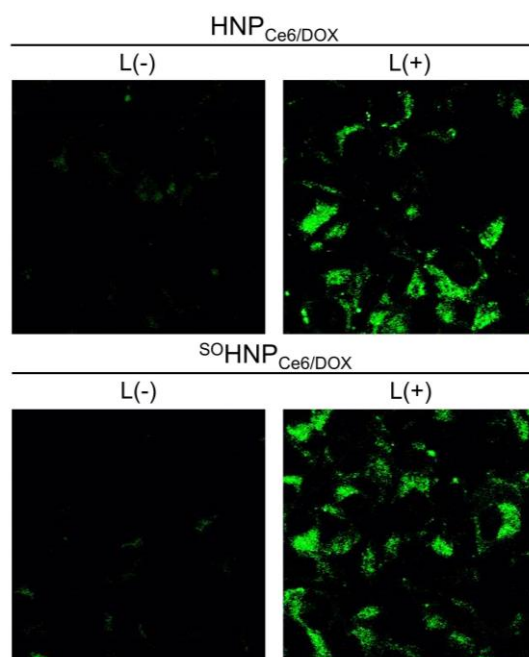


**Figure S11.** Fluorescence microscopy image of cells incubated with DCF-DA and then treated with  $\text{HNP}_{\text{Ce6/DOX}}$  and  $^{\text{SO}}\text{HNP}_{\text{Ce6/DOX}}$  with or without 660 nm laser irradiation ( $0.2 \text{ W/cm}^2$ , 15 min).

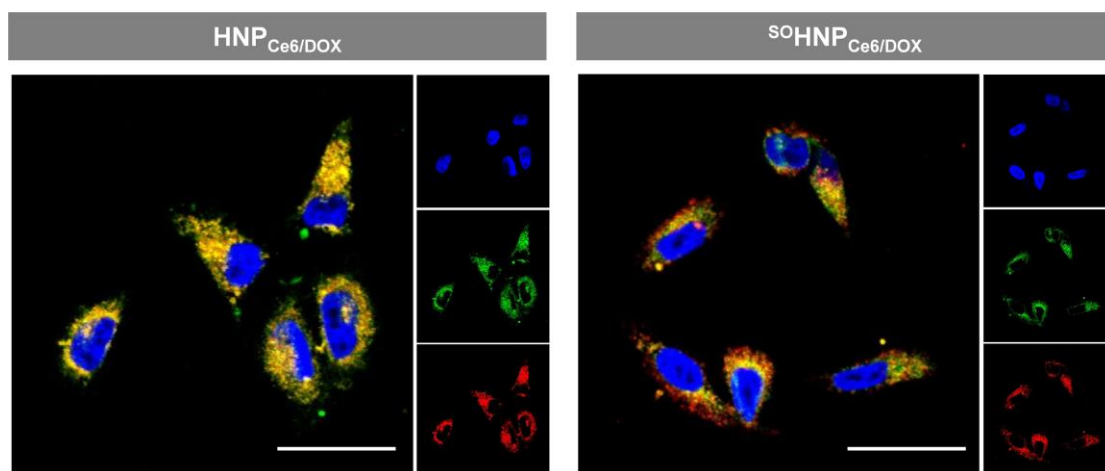


**Figure S12.** Assessment of the intracellular DOX release and biodistribution of  $\text{HNP}_{\text{Ce6/DOX}}$  or  $^{\text{SO}}\text{HNP}_{\text{Ce6/DOX}}$  in MCF-7/ADR cells without continuous 660-laser irradiation ( $0.1 \text{ W/cm}^2$ ). The concentration of DOX in the cell culture was  $6 \mu\text{g/mL}$ . Acidic endosomes/lysosomes and cell nuclei were stained with LysoTracker<sup>TM</sup> Green

(green) and DAPI (blue), respectively.

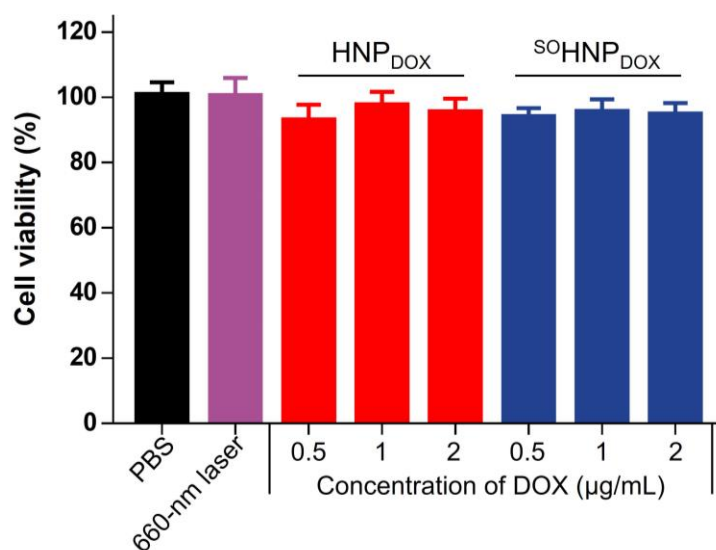


**Figure S13.** Cytotoxicity of laser, HNP<sub>DOX</sub> and <sup>SO</sup>HNP<sub>DOX</sub> against MCF-7/ADR cells for 72 h. The power density of 660-nm laser (NIR) was 0.1 W/cm<sup>2</sup>.

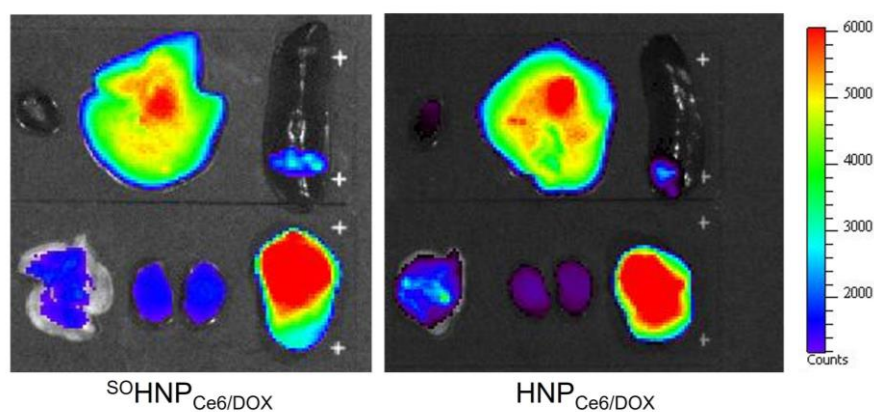


**Figure S14.** Fluorescence image of Ce6 in major organs 24 h post systemic injection. The quantification of fluorescence intensity calculated by the software is shown in Figure 6C and 6D.

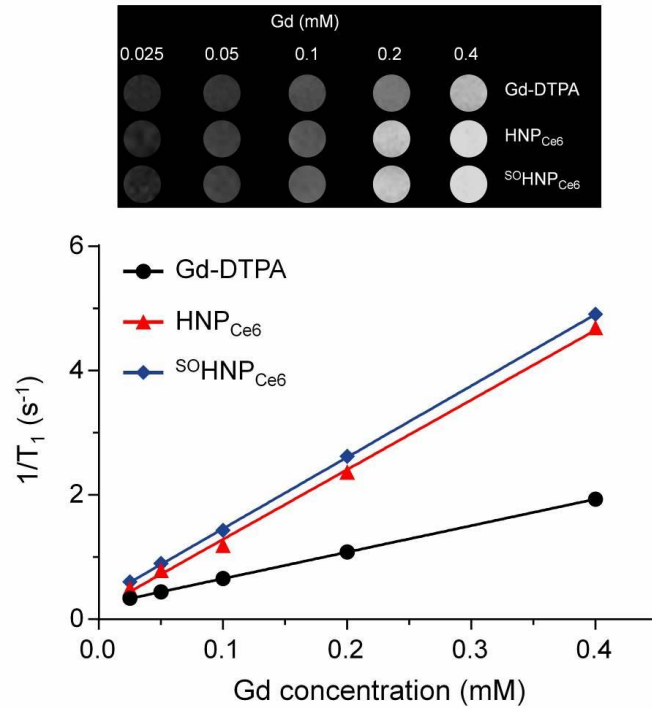


**Figure S15.** Water proton longitudinal relaxation rate ( $1/T_1$ ) of HNP<sub>Ce6</sub> and SOHNP<sub>Ce6</sub> in aqueous solution as a function of  $Gd^{3+}$  concentration. The small molecular Gd-DTPA complex was used as a control.

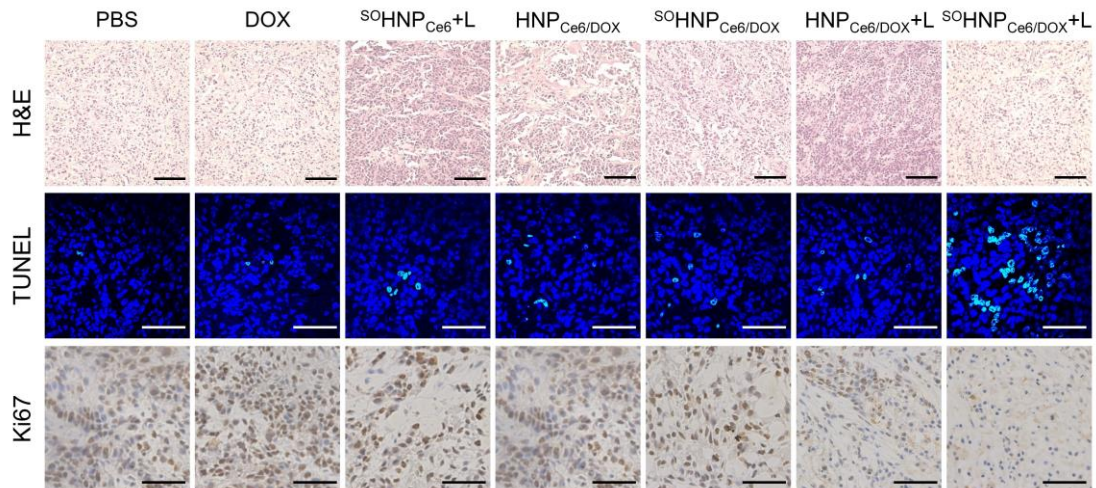


**Figure S16.** H&E, TUNEL and Ki67 analyses of tumor tissues from mice treated with the indicated formulations. The scale bar for H&E analyses was 200  $\mu m$ . The scale bar for both TUNEL and Ki67 was 100  $\mu m$ . Ki67-positive proliferating cells are stained brown.

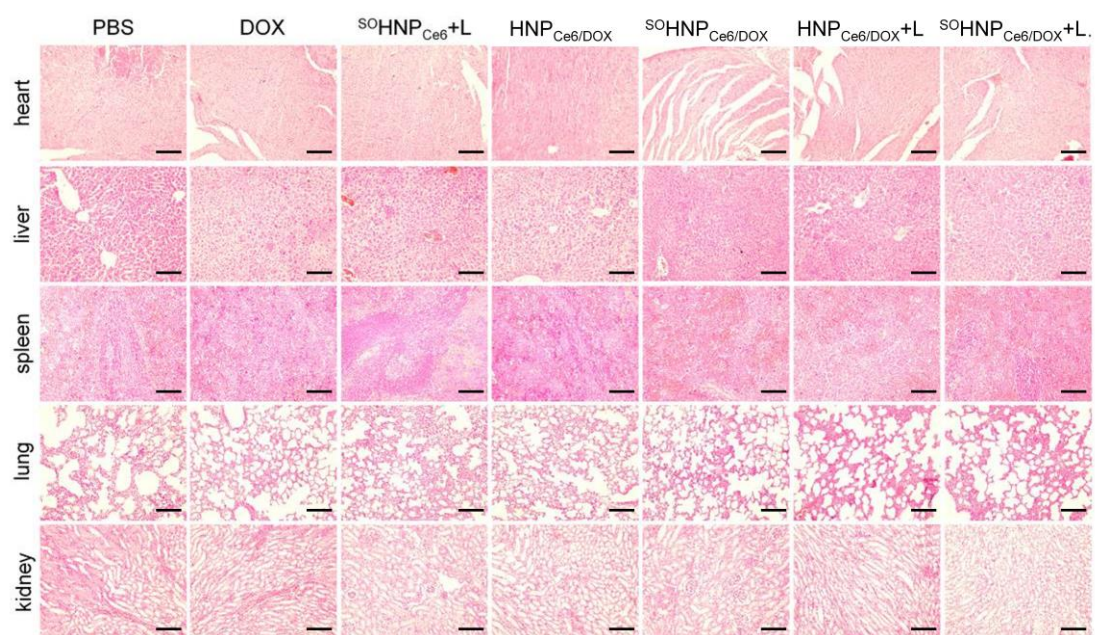


**Figure S17.** Histopathology analyses of visceral organ sections from MCF-7/ADR xenografted female mice after the tumor growth inhibition experiment (scale bar: 200  $\mu\text{m}$ ).

PBS (1) DOX (2)  $^{50}\text{HNP}_{\text{Ce6}}+\text{L}$  (3)  $\text{HNP}_{\text{Ce6}/\text{DOX}}$  (4)  $^{50}\text{HNP}_{\text{Ce6}/\text{DOX}}$  (5)  
 $\text{HNP}_{\text{Ce6}/\text{DOX}}+\text{L}$  (6)  $^{50}\text{HNP}_{\text{Ce6}/\text{DOX}}+\text{L}$  (7)

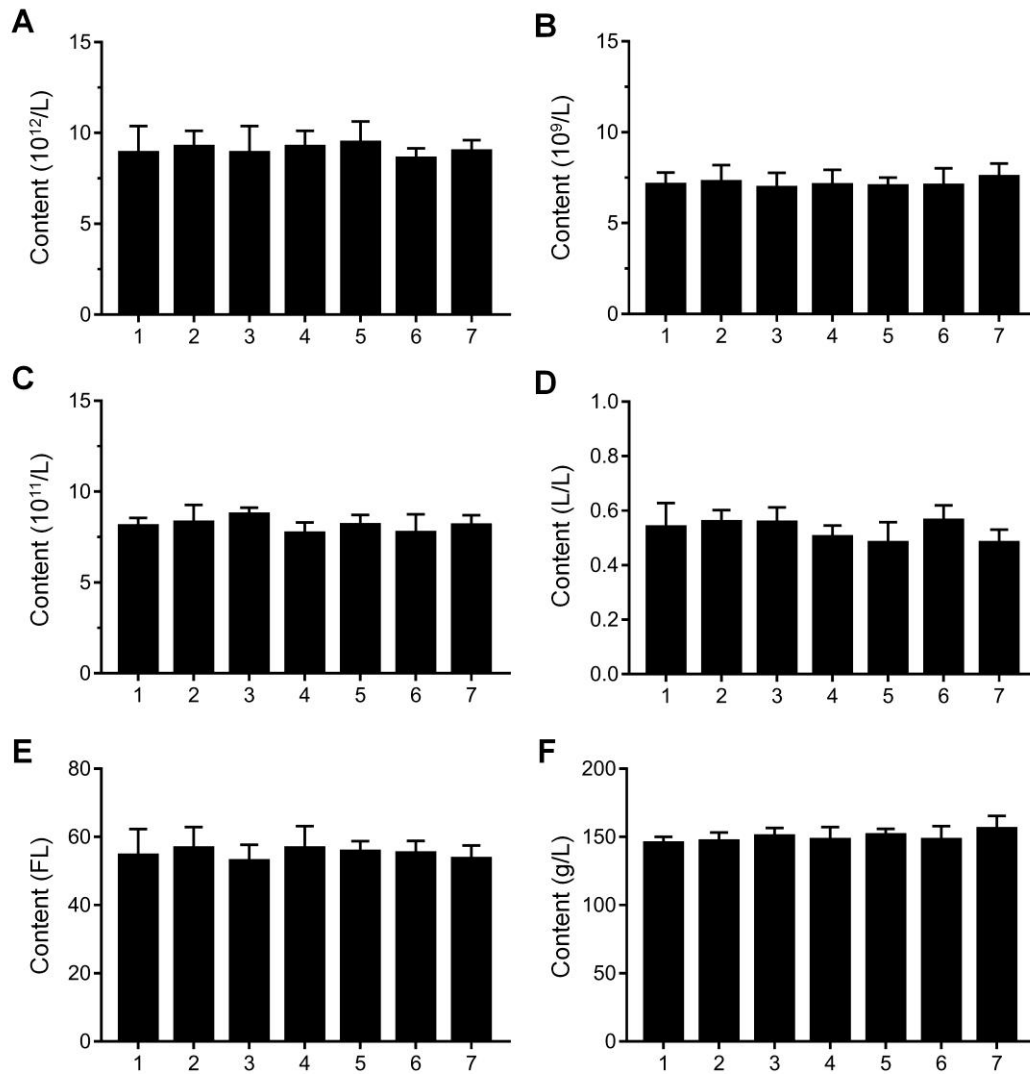


**Figure S18.** Hematology analysis of the mice after different treatments: (A) red blood cell (RBC), (B) white blood cell (WBC), (C) platelet (PLT), (D) hematocrit (HCT), (E) mean corpuscular volume (MCV), and (F) hemoglobin (HGB), respectively.

**Table S1.** Drug loading content (DLC) and encapsulation efficiency (EE) of Ce6 and DOX for <sup>SO</sup>HNP and HNP.

Parameter	DLC (%)		EE (%)	
	Ce6	DOX	Ce6	DOX
HNP <sub>Ce6/DOX</sub>	3.51	3.27	35.1	32.7
<sup>SO</sup> HNP <sub>Ce6/DOX</sub>	3.39	3.13	33.9	31.3

**Table S2.** Pharmacokinetic parameters of these formulations after intravenous administration.

Parameter	AUC <sub>0-48h</sub> (µg/L*h)	t <sub>1/2z</sub> (h)	C <sub>max</sub> (µg/L)	CI
DOX	64.70	18.46	14.15	21.53
HNP <sub>Ce6/DOX</sub>	810.79	26.47	124.77	1.64
<sup>SO</sup> HNP <sub>Ce6/DOX</sub>	728.83	27.74	140.84	2.82

AUC, area under curve; t<sub>1/2z</sub>, elimination half-life; C<sub>max</sub>, peak concentration; CI, clear rate.